International Journal of Scientific Research and Modern Education (IJSRME)
ISSN (Online): 2455 – 5630 & Impact Factor: 3.110
National Conference on Recent Trends in Applied Chemistry (NCRTAC–2016)
Easwari Engineering College, Ramapuram, Chennai, Tamilnadu

SYNTHESIS, STRUCTURAL, OPTICAL AND DIELECTRIC PROPERTIES OF ZnS NANOPARTICLES FOR THE FABRICATION OF DSSCs

F. Michael Raj*, R. Sathish & A. Jeya Rajendran***
* Advanced Materials Research Lab, Department of Chemistry, Loyola College, Chennai, Tamilnadu
** Department of chemical engineering, CECRI, Karaikudi, Tamilnadu

Abstract:

Zinc sulfide nanoparticles were synthesized by chemical co-precipitation method from homogenous solutions of zinc nitrate and sodium sulfide in the presence of surfactant, tetrabutylammomium bromide (TBAB). The optical properties of surfactant-capped zinc sulfide nanoparticles were investigated using UV–visible absorption and photoluminescence spectral analysis. X-ray diffraction pattern of ZnS revealed the polycrystalline nature with cubic zinc blende structure and the grain size was calculated as 1.7 nm using Debye-Scherer method. The bandgap and optical size were calculated from the UV spectral data as 4.25 eV and 3.2 nm respectively. The morphology of ZnS nanoparticles were studied by Field emission scanning electron microscopic technique and their elements composition was confirmed by energy dispersive x- ray analysis (EDAX). Electrical properties of the as-synthesized ZnS nanoparticles were investigated by dielectric studies. The variation of dielectric constant, dielectric loss and AC conductivity studies were studied over a range of frequency (50 Hz to 5 MHz) and temperature (40 °C to 140 °C). Solar cell was fabricated using cadmium sulfide as photocathode material, TiO_2 - ZnS as photoanode material, potassium iodide / triiodide (KI/I_3^-) as an electrolyte solution, ruthenium red dye as a sensitizer and solar conversion efficiency was found to be 3.84%.

Key Words: Tetrabutylammonium Bromide, Solar Cell, Dielectric Constant & X-Ray Diffraction

1. Introduction:

Wide bandgap II-VI semiconductors especially ZnS is non-toxic, chemically more stable and important phosphor host material used in optoelectronic applications including photoconductors, solar cells, field effect transistors, sensors, transducers, optical coatings and light emitting materials[1-4] due to large band gap (3.7eV) and high refractive index (2.2) of the material. Generally, the nanoparticles exhibits variation in their properties to the bulk material due to two factors namely the increase in surface to volume ratio and change in electronic structure of the material by the quantum confinement effect [5-7].

The photoelectrical properties make ZnS nanoparticles as a very promising material in solar cell applications. ZnS nanoparticles have been synthesized through various methods including hydrothermal, micro-emulsion, sol-gel, chemical co-precipitation, sonochemical, microwave irradiation and solvothermal methods [8-12]. However these methods normally consist of two or more steps and rigorous conditions, such as high pressure or high temperature are required to attain nanoparticles [13]. The tunability of nanoparticles by controlling their size may provide an advantage of formulating new materials with optimized properties for various applications. However these applications would be restricted due to the nonradiactive pathways araising from

surface related defects. To overcome the above difficulties, organic, inorganic and polymer capping agents are used to passivate the free quantum dots [14]. To control the growth of ZnS nanoparticles organic capping agent was added during the synthesis of nanoparticles.

Chian Ko et al and Ashin Ko et al were used tetrabutyl ammonium bromide a surfacting agent to prepare Au and Pt nanoparticles[15,16]. Capping agents are frequently used in colloidal synthesis to inhibit nanoparticle overgrowth and aggregation as well as to control the structural characteristics of the resulted nanoparticles in a precise manner. The effect of the residual capping agents on particle surface has unveiled various adverse and favorable behaviors in catalytic applications. The electronic properties of polycrystalline materials consisting of small crystallites have been investigated in semiconducting material like ZnS, the study of electrical conductance in system consisting of nanoparticles is very limited and hence there is a scope for further studies on electrical properties of pelletized ZnS nanoparticles as semiconductors would be an interesting area of materials research.

In this paper, the ZnS nanoparticles were synthesized by chemical precipitation method at room temperature with tetrabutylammonium bromide as a capping agent for controlling the particle size and used as photoanode material for dye sensitized solar cell for efficient power conversion energy.

2. Experimental Section:

2.1. Synthesis of ZnS Nanoparticles:

ZnS nanoparticles were synthesized by mixing 50 mL of 0.01M TBAB with 50 mL of 0.1M zinc nitrate solution in 250 mL round bottom flask and stirred for 30 min to get homogeneous transparent solution. 50 mL of 0.1M sodium sulfide solution was added drop wise to the mixture of zinc nitrate under continuous stirring until the formation of white precipitate was complete and the stirring was continued for 3 h. The chemical reaction is

$$Zn(NO_3)_2 + Na_2S \xrightarrow{TBAB} ZnS + 2NaNO_3$$

The solution was kept for 3 h to settle down the particles and separated by filtration. The precipitate was washed by suspending them in ethanol and centrifuged. The dried samples were ground using mortar and pestle to make fine powder for better characterization.

2.2. Instrumentation:

The optical absorption spectrum was recorded by using **Jasco V-700** series UV-vis spectrophotometer in the range of 200 to 800 nm. The Photoluminescence spectrum of the sample was obtained by using Perkin –Elmer LS 55 fluorescence spectrophotometer. XRD was recorded by Philips X' pert X-ray diffractometer using CuK_α radiation (λ= 0.154 nm) at 40 kV and 30 mA from 20º to 70º. The composition of nanomaterials was determined by energy dispersive X-ray analysis (EDZ, HITACHI S2400). The surface morphology was analyzed by spectrometer coupled with field emission scanning electron microscope (SEM, JEOL JSM 6360). Dielectric studies of the samples were investigated by HIOKI-Hi-TESTER 3532 LCR meter as the function of frequency 50 Hz – 5 MHz at temperature ranges from 40º - 140 ºC. I-V characteristics are measured by using YOKOGAWA GS610 Source Measure Unit.

2.3. Fabrication of Solar Cell:

2.3.1. Preparation of Photoanodes:

a) Synthesis of TiO_2 Nanoparticles: TiO_2 nanoparticles were synthesized from titanium isopropoxide, isopropanol and distilled water by hydrolysis reaction. Ammonia

was added to the mixture to maintain pH of the solution.The reaction mixture was stirred for 6 h to form the blue white precipitate of TiO_2 nanoparticles. The sample was filtered, centrifuged and dried to ontain pure white powder.

b) Synthesis of ZnS Nanoparticles: To prepare TiO_2 photoanode, the FTO sunstrates were cleaned and dried with acetone. The synthesized ZnS and TiO_2 powders were made into paste with acetone / water using mortor. The paste was applied on the FTO substrate by doctor blade method and heated at 250 °C for 3 h inorder to remove the organic substances.

2.3.2. Preparation of Photocathode:

CdS nanoparticles were synthesized by using cadmium acetate and sodium sulfide using precipitation method. The CdS powder was made into paste with acetone and water. The paste was applied on cleaned and dried FTO substrate by doctor blade method and dried in an oven for 3 h.

2.3.3. Fabrication of DSSCs:

Finally, the prepared TiO_2-ZnS photoanodes ($0.25cm^2$) were immersed in commercially available Ruthenium dye for 10 min and dried at 250 °C in an oven for 3h. Then, the sensitized photoanodes and CdS photocathodes were assembled and internal space was filled with an iodide/triiodide redox electrolyte. The cell current was measured by using Source measure unit and values were recorded.

3. Results and Discussion:

3.1. Structural Studies:

Fig.1 represents the XRD pattern for the TBAB capped and uncapped ZnS nanoparticles respectively. The obtained XRD patterns were well matched with those of ICDD file no.65-1691 [17]. The intensities of these major peaks of ZnS, namely (111) (220) and (311) reflections corresponding to 28.5º, 47.6º and 56.4º respectively. The lattice parameter is determined as 5.27 Å for pure and 5.36 Å for capped, which is very close to the standard value (5.42 Å). It is clearly observed the peak broadening of XRD pattern indicates the formation of ZnS nanoparticles and crystallite sizes are 2.74 nm for uncapped ZnS, 1.7 nm for TBAB capped ZnS nanoparticles. From the Fig.2. it is seen that peaks broadened for higher concentration of capping agent. The broadening of peaks indicates nanocrystalline behaviour of the particles. The crystallite size was determined from the width of first peak (111) using Debye Scherrer formula [17] and from Table.1. it is also observed that in the increasing capping agent concentration decreases the crystallite size of ZnS nanoparticles.

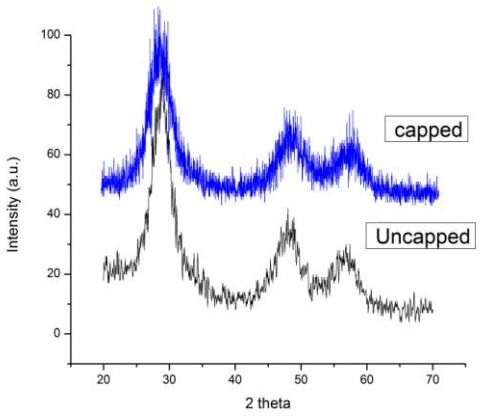

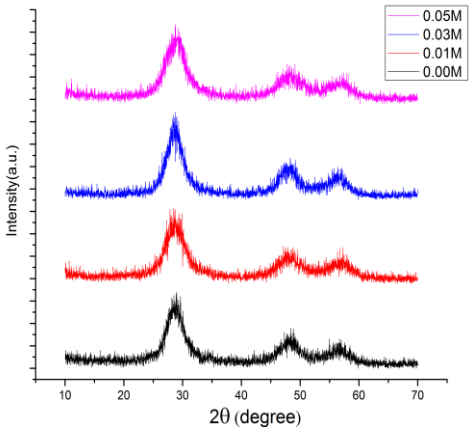

Figure 1: XRD pattern for pure and TBAB capped ZnS & Fig.2. XRD pattern for pure and TBAB capped ZnS with different molar concentration

Table.1. Calculated size of TBAB capped ZnS nanoparticles from Scherrer formula

Sample	Conc. of TBAB	Mean Crystallite Size (nm)	Band gap (eV)
ZnS (A)	0.0 M	2.74	4.19
ZnS(B)	0.01 M	1.89	4.21
ZnS(C)	0.03 M	1.82	4.22
ZnS(D)	0.05 M	1.72	4.25

3.2. Field Emission Scanning Electron Microscopy (FESEM):

FESEM is a powerful tool to study the surface morphology of the nanoparticles especially by observing the top and cross-sectional views. Fig.3. shows the FESEM image of synthesized pure and capped ZnS nanoparticles at 12,000 times magnification. The FESEM micrographs showed that the pure and TBAB capped ZnS nanoparticles have considerable agglomeration with less spherical morphology. EDAX spectral analysis confirms the presence of zinc and sulfur. The other small signals including carbon and oxygen which were due to sputter coating of glass substrate.

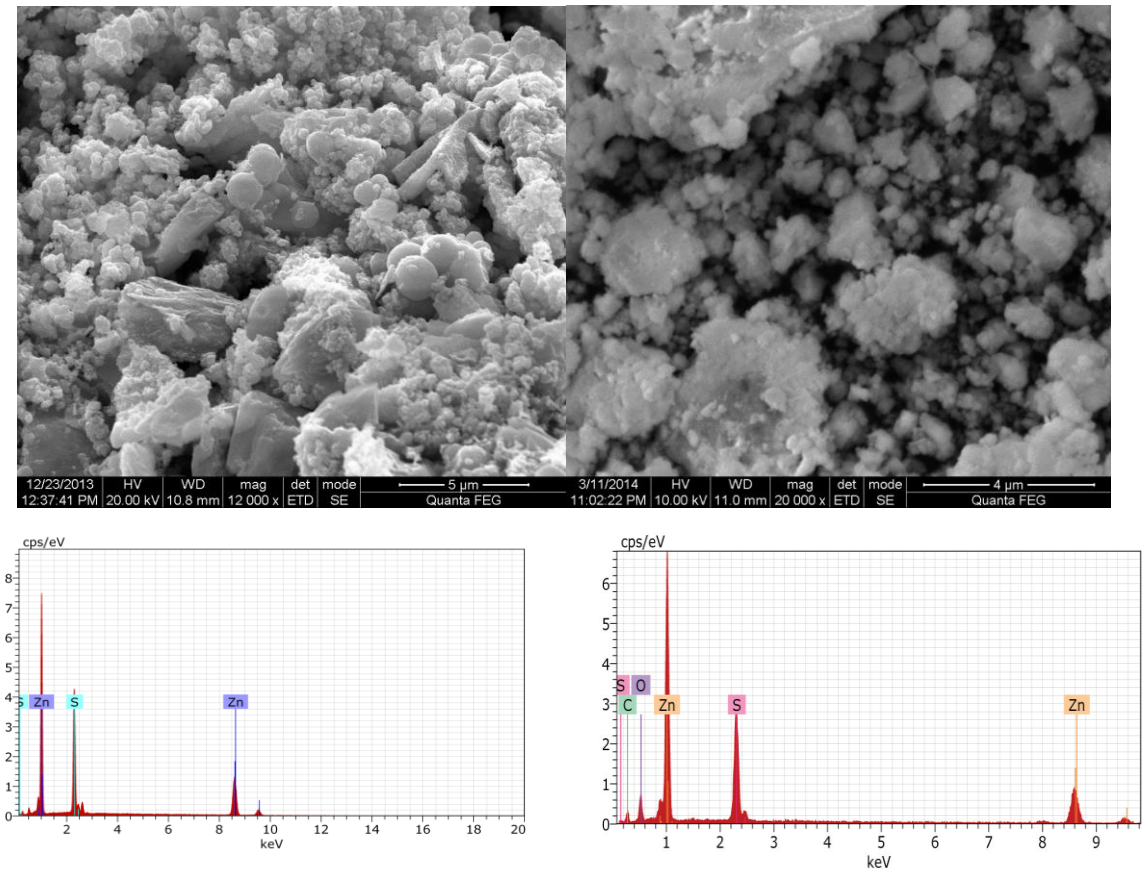

Figure 2: FESEM images and EDS spectra for pure (a and c) and TBAB capped ZnS (b and d)

3.3. Optical Studies:

Fig.3 shows the absorption spectra of TBAB capped and uncapped ZnS nanoparticles. The absorption peaks were obtained for 308 nm for uncapped, 285 nm for capped ZnS nanoparticles. The blue shift of absorption edge compared to bulk ZnS clearly explained by quantum confinement effect of ZnS nanoparticles. The optical size of ZnS was calculated using following eqn,[15,16]

$$\Delta E = \frac{\pi^2 h^2}{2\mu r^2} - \frac{1.78e^2}{\varepsilon_r} \quad \text{------(1)}$$

Where ΔE is band gap, μ is the reduced mass of electron, r is the cluster size, h is the planck's constant, ε_r is the dielectric constant.The first term indicate confinement effect and second term being columb term. As in the present case second term is too small since the charge of electron is negative value (1.6×10^{-19}c) and can be neglected. Compared to capped, uncapped ZnS absorbs at the largest wavelength peak at 308 nm with corresponding crystallite size of 2.8 nm however, for the capped ZnS absorption peak was observed at 285 nm.The bandgap energy was also calculated using UV-vis spectra by the relation,

$$(\alpha h\nu) = A(h\nu - E_g)^n \quad \text{------(2)}$$

Where, α is the absorption co-efficient, hv is the incident photon energy, A the constant and E_g bandgap energy. The taue plot is plotted by taking (αhv) vs (hv) , from the graph bandgap was calculated, which is listed in Table.2.

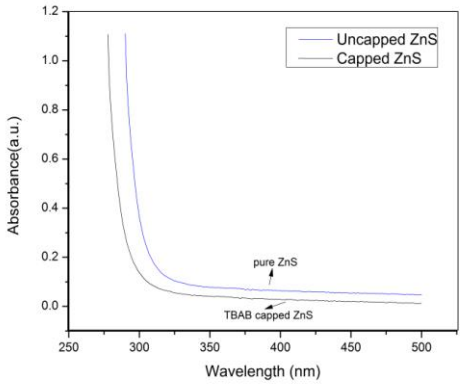

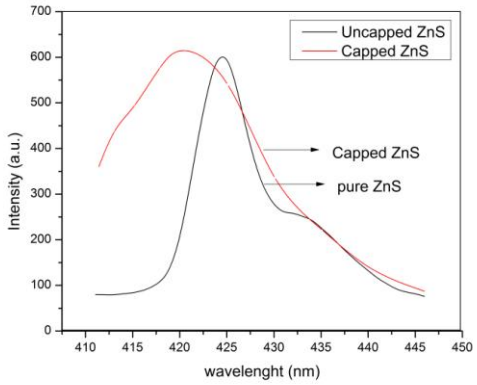

Figure 3: UV-vis spectra for pure and TBAB capped ZnS & Figure 4: PL spectra for pure and TBAB capped ZnS

The photoluminescence spectra of pure and capped ZnS nanoparticles were measured at room temperature and is shown in Fig.4. Comparing the PL spectra of TBAB capped and uncapped ZnS nanoparticles, PL spectra of the capped particle is broad i.e. shifted to 417 nm and for the uncapped ZnS nanoparticles the peak emission was at 425 nm.

Table.2.Crystallite size from UV and XRD pattern

Sample	Band gap (E_g) (eV)	Optical size in UV (nm)	Particle size in XRD (nm)
Uncapped ZnS	**4.19**	**3.4**	**2.74**
Capped ZnS	**4.25**	**3.2**	**1.72**

3.4. Dielectric Studies:

Dielectric studies of the bulk materials shows the effects of temperature and frequency on the conduction phenomenon in nano structured materials. Dielectric studies were carried out with a help of HIOKI 3532-50 LCR Hi TESTER model LCR meter as a function of frequency ranges from 50 Hz to 5 MHz at the temperature range of 40-140 ºC. The bulk material was taken in the form of disc of diameter 13 mm and thickness 0.8 mm for capped ZnS. The dielectric constant (ε_r) has been calculated using the following equation,

$$\varepsilon_r = Cd / \varepsilon_o A \quad \text{----(3)}$$

Where C is the capacitance, d is the thickness of the sample, ε_o is the permittivity in free space (8.856 x 10^{-12} $C^2N^{-1}m^{-2}$) and A, is the area of the sample. The results suggest that the dielectric constant (ε_r) and dielectric loss (tan δ) strongly depend on the frequency of the a.c. signal and the different temperatures of the ZnS nanoparticles. The dielectric constant has higher values in the lower-frequency (50 Hz) and then it decreases up to the high frequency (5 MHz). Most of the atoms in the nanocrystalline materials reside in the grain boundaries, which become electrically active as a result of charge trapping. The dipole moment can easily follow the changes in the electric field, especially at low frequencies.

Hence, the contributions to the dielectric constant increase through space charge and rotation polarizations, which occur mainly in the interfaces. Therefore, the dielectric constant of nanostructures materials should be larger than that of the conventional materials [15]. One of the reasons for the large dielectric constant of nanocrystalline materials at sufficiently high temperature is the increased space charge polarization due to the structure of their grain boundary interfaces. Also, at sufficiently high temperature the dielectric loss is dominated by the reason for the sharp increase of the dielectric constant at low frequencies and at lower temperatures. As the temperature increases, the space charge and ion jump polarization decrease, resulting in a decrease in the dielectric constant. In dielectric materials, dielectric losses usually occur due to the loss of energy on heating in a various applied electric field. The orientation of the molecules along the direction of the applied electric field in polar dielectrics requires a part of the electric energy to overcome the forces of internal friction.

Another part of the electric energy is utilized for rotations of the polar molecules and other kinds of molecular transfer from one position to another, which also involve energy losses. In nanophase materials, the grain boundaries have an amorphous or glassy structure [14]. All the inhomogenities, defects, space charge formation etc. together produce an absorption current, which results in dielectric losses. Due to the presence of the dangling bonds on the surface layers, the nanoparticles will be highly reactive, and there is a chance of adsorption of gases like oxygen or nitrogen. These adsorbed gases can also cause an increase in the dielectric loss. In nanophase materials, inhomogeneities like defects and space charge formation in the inter phase layers produce an absorption current resulting in a dielectric loss. Fig.5c shows the variation of the dielectric loss with respect to the logarithm of frequency at different temperatures of 40°C, 100°C, and 140°C. Dielectric loss also shows a trend similar to the one shown by the dielectric constant. The decrease in the dielectric loss with the increase in frequency for all the temperatures suggests that the dielectric loss is strongly dependent on the frequency of the applied field.

3.5. I-V Characteristics Studies:

Fig.6. indicates the photo current density versus voltage (J-V) transfer, showing the characteristics of fabricated solar cell device, 0.25 cm^2 in size. The cell was fabricated by coating titanium oxide, zinc sulfide and cadmium sulfide material on FTO glass by doctoral blade method. Ruthenium N719 red dye was used as a sensitizer in potassium iodide / iodine electrolyte solution. The short current density (J_{sc}), open circuit voltage (V_{oc}), fill factor (FF) and power conversion efficiency were found to be 5.4 mA/cm^2, 0.45 V, 0.37 and 3.84% respectively. This conversion efficiency was high compared to bare ZnS and TiO_2 photo anode materials. This conversion efficiency is yet

to be improved by replacing photoanode materials and by synthesizing different morphological structures of ZnS.

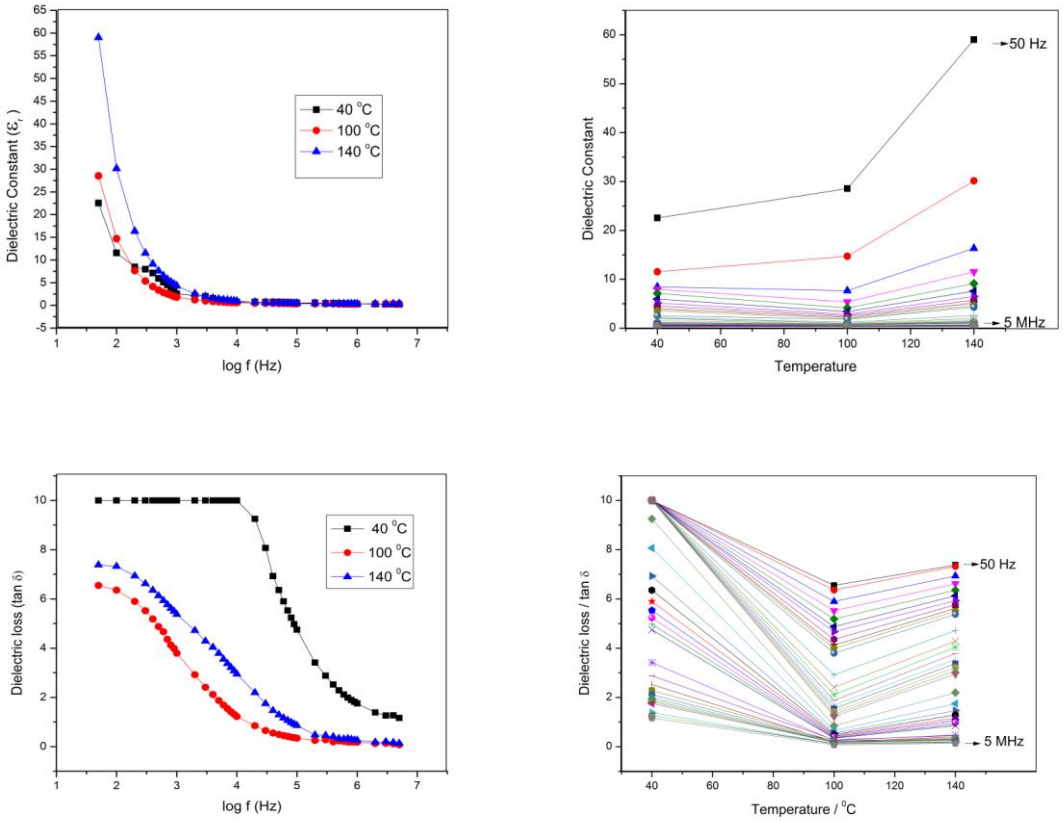

Figure 5: Dielectric constant and dielectric loss verses frequency at various temperatures

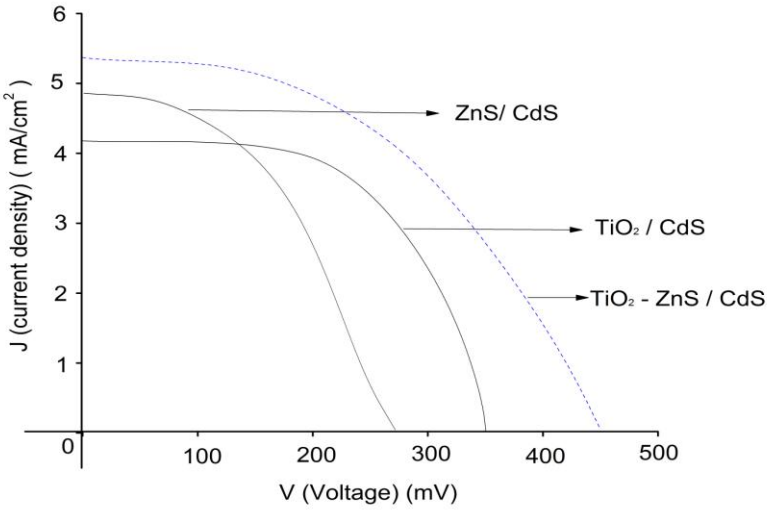

Figure 6: J-V characteristics of dye sensitized solar cell using ZnS, TiO_2 and ZnS-TiO_2 nanoparticles

Table 2: Photovoltaic parameters of the DSSCs based on bare ZnS, TiO_2, ZnS coated TiO_2 photoanode

Photoanode	**Photocathode**	**J_{sc} (mA cm^{-2})**	**V_{oc} (mV)**	**FF**	**η (%)**
ZnS	CdS	4.9	274	0.57	1.28
TiO_2	CdS	4.3	351	0.48	3.21
ZnS-TiO_2	**CdS**	**5.4**	**455**	**0.37**	**3.84**

4. Conclusion:

Nanoparticles of zinc sulfide have been synthesized via low cost, easiest, high yield precipitation method. It is found to be stable as there is no visible color changes over a period of month, if the nanoparticles were kept in dark condition wrapped with aluminum foil. The broad peak of the XRD pattern indicates nanocrystalline behavior of the particles. The dielectric properties like dielectric constant and dielectric loss have been studied. The TBAB capped ZnS possessed comparatively low dielectric constant since micro electronics industry needs low dielectric constant materials for various electro-optic devices and their applications. The ZnS coated TiO_2 photoanode in DSSCs shows more conversion efficiency of 3.84% than the bare ZnS (1.28%) and TiO_2 (3.21%) photoanode has been acheived with Ruthenium dye as sensitizer, KI/I_3^- electrolyte and CdS as a photocathode material. And further optimization of the photoanode by controlling the ZnS morphology, thickness and fabrication techniques will improve the efficiency for DSSCs, which is in progress in our laboratory.

5. Acknowledgement:

The authors greatfully acknowledges the financial support provided by UGC (India) in the form of a major project (**F.No.41-1005/2012(SR**)) providing necessary characterization facilities.

6. References:

1. J.Jie, W.Zhang, I.Bello, C.Lee and S.Lee, "One-dimensional II – VI nanostructures: Synthesis, properties and optoelectronic applications" Nano today, vol.5, pp 313-336, 2010.
2. Abbas Rahdar, "Effect of mercaptoethanol and Na_2S dropwise addition rate on zinc sulfide semiconductor nanocrystals:syhthesis and characterization" J.Nanostruct.Chem 3:61,2013.
3. M.Mary Jaculine, C.Justin Raj, Hee Je kim, A.Jeya Rajendran ,S.Jerome Das "Zinc Stannate nanoflower(Zn_2SO_4)photoanodes for efficient dye sensitized solar cells" Materials science in semiconducting processing, 2014 .
4. G.Murugadoss, M.Rajesh Kumar "synthesis and optical properties of Ni^{2+} doped ZnS nanoparticles" Appl.NanoSci.2012.
5. N.S.Nirmala Jothi, et al. "Investigation of one pot hydrothermal synthesis, structural and optical properties of ZnS quantum dots" material chemistry and physics 138: 186- 191 (2013).
6. A.V.Ubale and D.K.Kulkarni D , "Preparation and study of thickness dependent electrical characteristics of ZnS thinflims" Bulletin of material science , 28, 43-47 (2005).
7. Chen.H; Shi.D; Qi, J; Jia J, Wang,B ,"The stability and electronic properties of wurtzite and zinc blend ZnS nanowires" Phys.lett.A. 371-375 (2009).
8. Ding,Y; Wang X.D; Wang ,Z.C; "Phase controlled synthesis of ZnS nanobelts: zinc blende wurzite, Chem, Phys.lett, 398, 32-36, (2004).

9. Rita John, S; Sasi Florence,"Optical , structural and morphological studies of bean-like ZnS nanostructures by aqueous chemical method" Chalcogenide letters 269-273 (2010).
10. Baoyou Geng, Jnzhu Ma , Fangming Zhan , Mat. Chem and Phy 534, 113,(2009).
11. Toshibiro Kuzuya et al. "Synthesis of ZnS nanocrystals and fabrication of nanocrystal superlattice"Materials transantions, 45: 2650-2652 (2004).
12. Rabidar , V. Arababi and H.Ghambori, "Study of electro optical properties of ZnS nanoparticles prepared by colloidal particles method" , World Academy of Science Engineering and Technology 6 (2012).
13. Hao Ying Lu, Sheng Yuan Chu and Soon-seng Tan, "The characteristics of low temperature synthesized ZnS and ZnO nanoparticles", Journal of crystal growth 269, (2004).
14. Nell, J, Marohn, G. Melendon J.Chem .Phys.94: 4359 (1990).
15. Spanhel, M, Haase, H. Weller, A, Hehglein , J .Am.Chem .Soc. 109: 5649 (1987).
16. SHE Yuan-Yuan, Yang –Juan, Qiuke Qiang "Synthesis of ZnS nanoparticles by solid – liquid chemical reaction with ZnO and Na_2S under ultrasonics" Tran's .Met. Soc. China 20: 5211-5215 (2010).
17. Patterson, A , "The scherrer formula for X- ray particle size determination", Phy. Rev. 56: 978 (1939).